Role of density in granular lubrication

A. J. Batista-Leyva*
CINVESTAV-Monterrey, Autopista Nueva al Aeropuerto Km. 9.5, Apodaca, Nuevo León 66600, México

F. Pacheco-Vázquez
Departamento de Física Aplicada, CINVESTAV-Mérida, A. P. 73 Cordemex, Mérida, Yucatán 97310, México

J. C. Ruiz-Suárez
CINVESTAV-Monterrey, Autopista Nueva al Aeropuerto Km. 9.5, Apodaca, Nuevo León 66600, México
(Received 9 March 2010; revised manuscript received 23 June 2010; published 8 September 2010)

We investigate the dynamics of a disk shaped intruder sliding on a granular monolayer. The monolayer is on an inclined transparent plane, tilted at an angle much smaller than the angle of avalanche. A high speed camera allows us to measure the dynamics of both, the intruder (filming from top) and the grains (filming from below). We find a frictional force with a dependence on the speed of the intruder. Moreover, calculating a Reynolds-like number, it is possible to highlight the influence of the density of the beads that form the monolayer on the dynamics of the disk. We also find that the fluidization produced by the intruder's action reduces substantially the effective friction coefficient.

DOI: 10.1103/PhysRevE.82.031304 PACS number(s): 45.70.−n, 05.70.Fh, 05.70.Ln, 05.70.Np

I. INTRODUCTION

Although friction is an omnipresent force in nature, the science in charge to understand it, tribology, is still full of challenges. This is especially true in granular systems, where friction emerges as a collective phenomenon. A granular monolayer resting on a flat plane is a prime example where the equilibrium condition of the system is indeed set by friction forces. Several groups have contributed to clarify this subject. Dorbolo [1] and Scheller *et al.* [2] measured the stability and critical angle of a monolayer of this kind located on a flat rectangular surface, when tilted about one of its sides. In their measurements a loose packed monolayer is created, and they study the time and spatial evolution of the heap. They found a behavior that can be modeled by stop-and-go motions of separated areas of the heap. The influence of the Jansen like friction, especially when the heap is narrow, indicates the arching in the bed. Other authors [3] studied the Pouiselle flow of a granular bed in an inclined channel, and found that it is related with the geometric characteristics of the channel. They discovered two regimes, one of them with high particle density, long range correlation and local ordering, and a dilute one, with long mean free path, and almost collision free. Candelier and Dauchot [4] performed an experimental investigation of the movement of a cylindrical object, dragged by a constant force, in a monolayer of cylinders of smaller radius vibrated horizontally in a direction perpendicular to the object's displacement. They found some interesting features when the packing fraction is close to the jamming transition, which separates two different regimes of motion: below the transition, the rearrangements in the cylinders dominates the intruder's dynamic, while above the transition the motion takes the form of chainlike structures, suggesting the dominance of the stress fluctuations.

In order to understand the dynamics of the movement of a grain rolling on a pile, Quartier *et al.* [5] studied a model system: a cylindrical intruder rolling over a heap formed by an array of identical cylinders. In their work, an explanation of fundamental characteristics of granular flow in piles (hysteresis between flow and statics, and the almost constant velocity of the grains in the flowing regime) is based in the potential energy landscape of the heap, and in the balance of kinetics-potential energy.

Dry friction has also been studied in bi- and tridimensional granular ensembles, (gases and solids) [6–10]. In a recent work [11] Baldassarri and co-workers studied experimentally a granular medium sheared in a Couette geometry and showed that the statistical properties of the system can be computed assuming that the resultant from the set of friction forces acting in the system performs a Brownian motion.

Our group has recently studied the movement of an intruder through a channel filled with expanded polystyrene beads [12]. We were interested, above all, in understanding the influence of the density, speed of the intruder, and also the depth of the channel, in the final penetration distance. An interesting feature of its kinematics is the fact that the effective frictional force acting on the intruder does not seem to depend on its mass, as in the case of Coulomb friction of a sliding object down an incline. It was suggested that this could be related with the low density of the beads.

In the present paper we perform a systematic study of the dry friction between a granular monolayer and a disk moving on it. The beads we have used in this work are of three different materials (glass, tapioca, and expanded polystyrene) whose densities range from 2210 to 14 kg/m^3. We found a friction force that depends on the intruder's speed and the density of the beads. Since one normally takes for granted that a monolayer of spherical beads performs very well as a dry lubricant, our results imply that upon reducing the den-

*Corresponding author, On leave from Instituto Superior de Tecnologías y Ciencias Aplicadas, La Habana, Cuba; alfobatista@yahoo.com

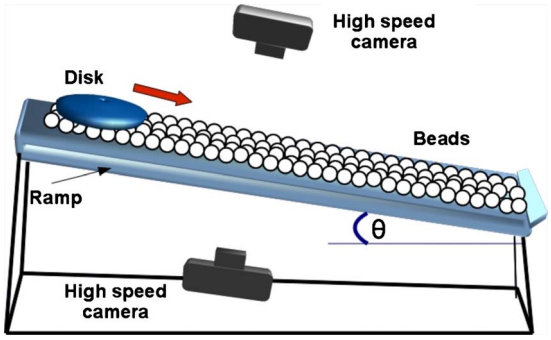

FIG. 1. (Color online) Schematic view of the experimental setup.

sity of the beads to a very low value, this lubrication performance excels.

II. EXPERIMENTAL SETUP

Figure 1 is a sketch of our experimental apparatus: a ramp, 1.20 m long $\times$ 0.05 m wide, with a Plexiglas plate in the bottom and aluminum side walls. In each experiment, the plate is covered with a monolayer of beads of one of three different materials previously named (see Table I for details). The monolayer is retained by a Plexiglas wall at the end of the incline.

At the top of the granular monolayer a cylindrical intruder (made of Plexiglas at the bottom, steel at the walls, and diameter 2.56 cm) rests against a removable Plexiglas wall (not shown in the figure). When freed, the intruder slides downhill above the monolayer. A charge coupled device (CCD) fast speed camera, which can be located below or above the ramp, records the pass of the intruder or the displacement of the beads. All the results shown here were obtained filming at 500 frames per second. When the camera is located above the ramp, it can follow the pass of the intruder almost in all the ramp extension, while when filming from below, 9.1 cm of the ramp is filmed, enough to follow the complete trajectory of individual beads as they move below the intruder.

The angle between the ramp and horizon is determined by a digital level. It can be changed in the range $(0°, 45°)$. Each experiment was carried out in the following way: the inclination of the ramp is fixed at a low angle and the beads are placed, then the angle is increased, while the ramp is been gently vibrated in order to obtain a dense packing. Each experiment was repeated three times. In Table I, γ_m represents the average packing of the unperturbed layer. γ_m is measured using the Analyze/Measurement option of ImageJ in the first frame of the videos recorded from bellow. The variation in the initial filling factor among different experiments with the same material is less than 2%. Once the angle is fixed, the intruder is liberated, starts to move and its trajectory is recorded. In Table I γ is the average packing below the intruder when moving down the incline, measured in the same way as γ_m, but limiting the scan to the area covered by the intruder. The area of the intruder is always the same and its mass varies between 1 and 56 g, changing the pressure over the beads. In this range of masses the expanded polystyrene beads barely deform. In fact, with the heaviest intruder used in this work (56 g) the measured deformation is 20 μm (measured when only 4 beads support the intruder), so the deformation of the beads in our experiments is much less than 0.4% of the diameter. The angle was varied between 2.1° and 15.6°. The static friction was measured in the following way: beads of the material under test (having radii that do not differ more than 0.1%) were glued to a flat surface and then placed on the empty ramp. Increasing the inclination of the ramp, the critical angle of sliding was measured. Measurements were repeated until the statistical component of uncertainty was 0.4°. The coefficient of static friction μ_s for the three materials is also shown in Table I. During the experiments, the humidity in the laboratory area was below 35%. To avoid static electricity (specially in the expanded polystyrene beads) antistatic spray was applied to the beads and the ramp between experiments.

III. RESULTS AND DISCUSSIONS

First, in order to obtain the acceleration of the intruder while it moves downhill along the incline we plot its position in the central axis of the ramp (x coordinate) as a function of time (Fig. 2). The data were taken at an angle of 13.7°. For the polystyrene beads the curves follow a perfect parabolic dependence for all the intruder masses, see Fig. 2(a), from which the acceleration can be calculated. However, for the other two materials the kinematics of the sliding intruder appreciably differ. While the more massive intruders follow an almost parabolic behavior, the lighter ones do not [see Figs. 2(b) and 2(c)], indicating a variable acceleration; its average value is easily estimated by fitting the data to a parabolic dependence. In Fig. 2(d) we plot x vs t for a large intruder mass (48.65 g) and the three materials. It is evident the greater acceleration and speed for polystyrene, followed by tapioca and then glass.

The above discussion is summarized in Fig. 3(a) where we show the dependence of the acceleration with the mass of

TABLE I. Characteristics of the materials.

Material	ρ (kg/m^3)	R_b (cm)	$\Delta R_b/R_b$ (%)	m (g)	μ_s	γ	γ_m	$\eta \pm \Delta\eta$ (kg/m)
Polyst.	14	0.263	5.7	0.001	0.56	0.760	0.860	0.004 ± 0.001
Tapioca	1180	0.156	5.1	0.019	0.42	0.507	0.745	0.042 ± 0.003
Glass	2210	0.149	2.7	0.032	0.38	0.856	0.890	0.064 ± 0.004

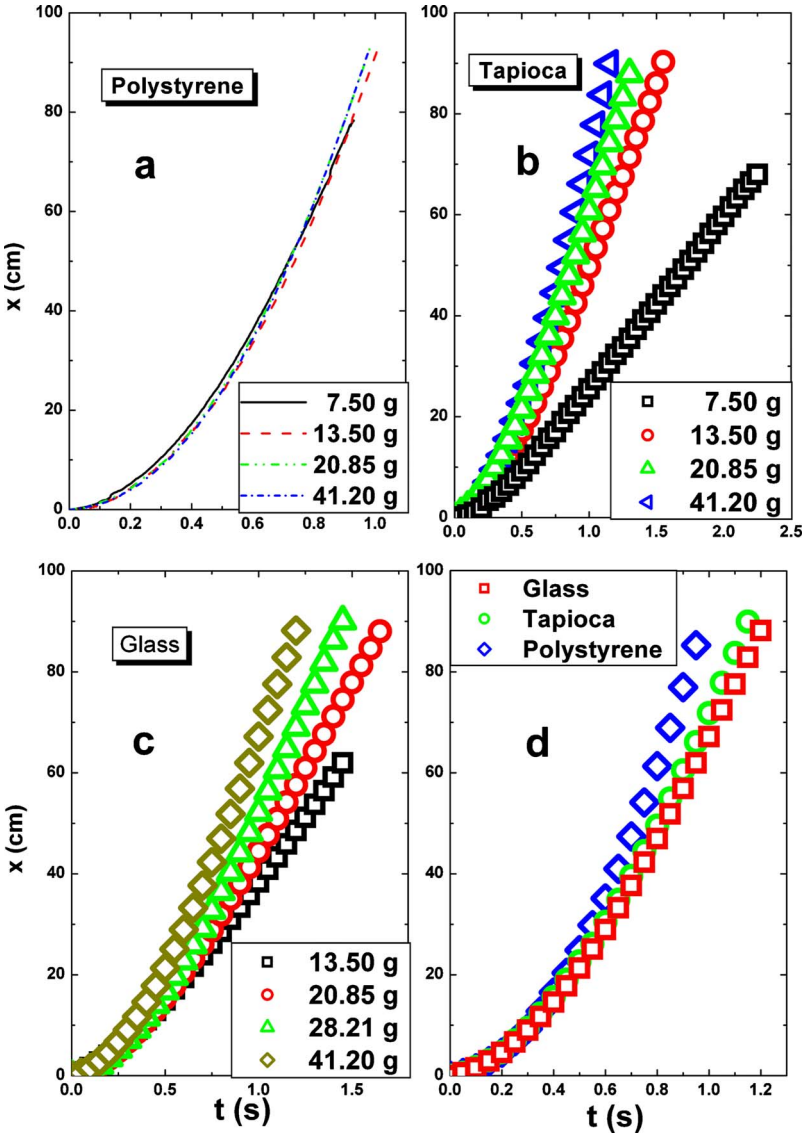

FIG. 2. (Color online) Kinematics of the intruder representing the displacement along the ramp vs time: (a) expanded polystyrene, (b) tapioca, (c) glass, and (d) comparative of the kinematics of the intruder for the three beads (with the mass of the intruder being 48.65 g).

the intruder for the three materials. It is very clear the remarkable difference in their behavior. While for tapioca and glass beads an approximately linear increase of acceleration is obtained, for polystyrene beads the curve first increases abruptly, then slows down a bit, saturates and finally shows a moderate decrease.

We learn from these results that for polystyrene beads, in some range of masses, the effective friction does not depend on the mass of the intruder or on its speed, as in a classic sliding experiment. Indeed, in this range of masses, the effective kinetic friction coefficient is $\mu_{eff}=0.046\pm0.007$, calculated accordingly to the following equation:

$$\mu_{eff} = \tan\theta - \frac{a}{g\cos\theta}. \quad (1)$$

Note that this is one order of magnitude smaller than the coefficient obtained in static friction experiments for the same material, see Table I.

The dependence of the acceleration with the angle at a constant mass (13.50 g) for polystyrene is shown in Fig. 3(b). A change in the slope for angles greater than 4° could be a fingerprint of the transition from pure rolling of the beads to rolling and sliding [13,14]; this possibility will be visited in a future work.

Figure 4(a) shows the velocity of the intruder (obtained by numerical derivation of the data) as a function of time for the three materials and for an intruder of low mass. Here, the details of the intruder's dynamics are clearly observed: while for glass and tapioca the speed reaches a terminal value, for polystyrene beads the intruder keeps an approximately constant acceleration. More massive intruders also give the same qualitative behavior, see Fig. 4(b). So, the acceleration of the intruder changes as it slides down the incline, and when we calculate the average acceleration its value also changes depending on the length of the incline considered.

The above results clearly imply that there is a friction force that depends on the speed. In order to understand this behavior we calculate the friction force f_r that acts on the intruder, considering that this is the sum of the interactions with n identical beads of mass m that roll on the incline below the intruder, but slide and roll between the intruder

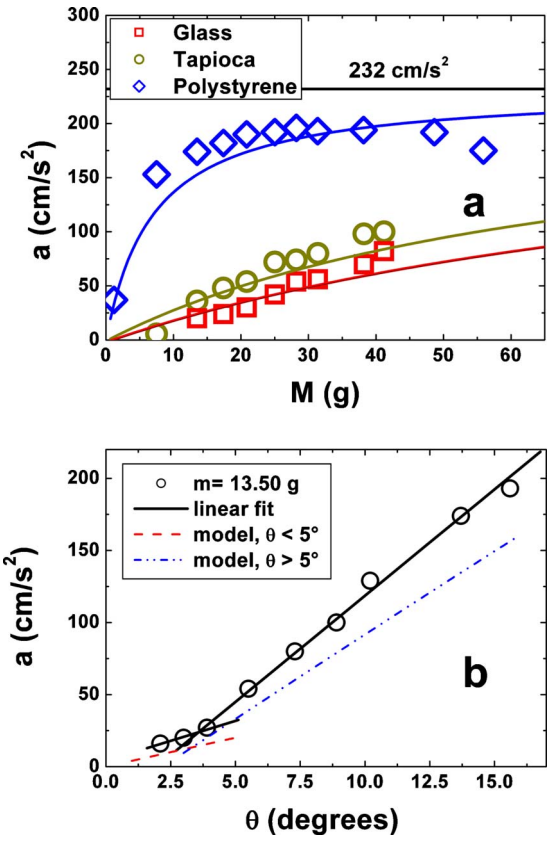

FIG. 3. (Color online) (a) Dependence of the mean acceleration of the intruder with its mass for the three materials. The lines are a representation of Eq. (11) (see text). The horizontal line represents the maximum attainable acceleration $g \sin \theta$. (b) Dependence of acceleration with the angle of the ramp for polystyrene beads. A change in the slope can be seen. Continuous lines are linear fits to the data; one in the region of small angles, the other for the larger angles. The dashed lines are a representation of Eq. (11), (see text).

and the beads. Calling f_{r1} to the friction force between the intruder and one bead, it follows:

$$f_r = n f_{r1}. \tag{2}$$

Taking into account this equation, and the theorem of work and energy for the displacement of one bead (see Appendix for details) we can find that the frictional force acting on the intruder is

$$f_r = \frac{7nm}{20\xi R} v^2 + \frac{nm}{2} g \sin \theta. \tag{3}$$

Here $\xi = \frac{R}{x_0}$ being R the radius of the intruder and x_0 the average distance that a bead travels while the intruder moves along the plane a distance R, v the intruder's speed, g the acceleration of gravity and θ the angle of inclination. From Eq. (3) we find that

$$f_r = \eta v^2 + M_b, \tag{4}$$

where

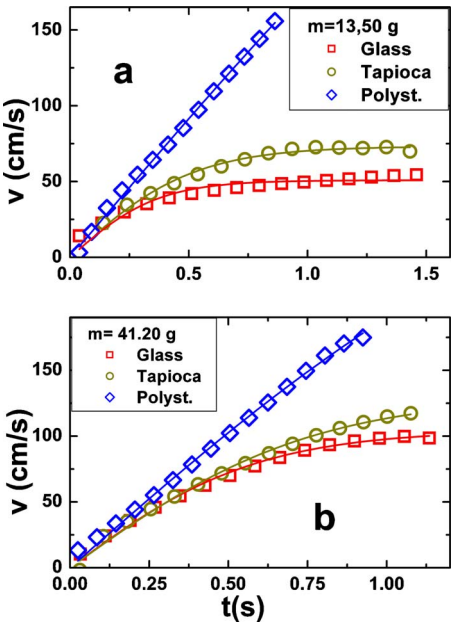

FIG. 4. (Color online) The speed of the intruder versus time. The full lines are a fit to Eq. (8), see text. (a) Mass of the intruder 13.50 g and (b) mass of the intruder 41.20 g. The angle in both cases is 13.7°.

$$\eta = \frac{7nm}{20\xi R} \tag{5}$$

or

$$\eta = \frac{7nmx_0}{20R^2}. \tag{6}$$

Any of the last two equations allows us to determine the drag coefficient η. $M_b = \frac{nm}{2} g \sin \theta$ is half the tangential component of the weight of the beads that are below the intruder. This is a constant component of the friction, and is always present. Its importance depends on the magnitude of η.

Taking into account these two facts, we propose a dynamic equation of the form:

$$M\frac{dv}{dt} + \eta v^2 = \kappa, \tag{7}$$

where $\kappa = (M - \frac{nm}{2}) g \sin \theta$ and M is the mass of the intruder. The quadratic dependence on the speed has been widely used in the analysis of data of the movement of intruders in granular media, for instance in [15] and references therein; here it arises naturally from the interactions of the intruder and the beads. The solution of Eq. (7) for intruders initially at rest is

$$v(t) = \sqrt{\frac{\kappa}{\eta}} \tanh\left(\frac{\sqrt{\kappa\eta}}{M} t\right). \tag{8}$$

Using Eq. (8) to fit the experimental data [see for instance the continuous lines in Figs. 4(a) and 4(b)], we found the values of κ and η. Although both of them can be calculated using the above expressions, it is interesting to note that their experimental values have a meaningful physical significance. Indeed, η must depend only on the materials forming the

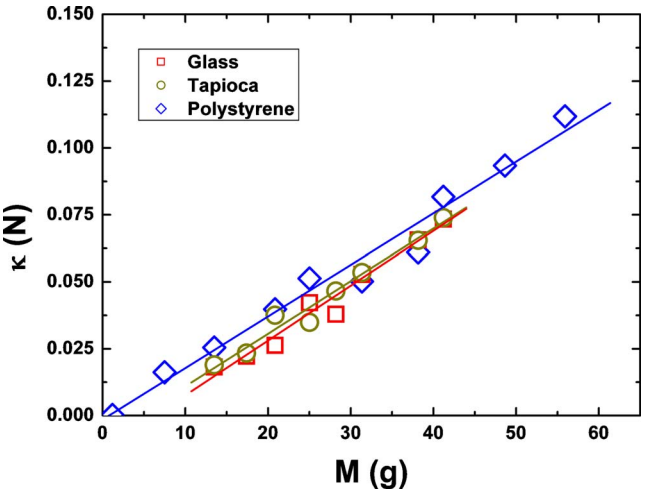

FIG. 5. (Color online) Dependence of κ with the mass of the intruder for the three materials. Continuous lines are a linear fit of the data.

monolayer, so when determining it from different intruder masses, the obtained values must be the same for each material. In Table I the experimental values of η are fairly constant. It is important to note that the value of η for the polystyrene beads is calculated for the experiments performed with an angle of 13.7°; for the smaller angles (below 4°) the value is around 0.22. Moreover, note that the coefficient for the polystyrene beads at 13.7° is an order of magnitude smaller than for the other two materials, so for such beads the friction dependence on the speed is not so important, in agreement with the findings of Fig. 4. We will later discuss the dependence of η on the properties of the beads.

Let us try now to understand the general behavior seen in the figures. In order to start moving for angles smaller than the critical one, the intruder must move the beads lying below. For the lighter particles this is easier, so the movement starts at very small masses. At the same time, due to the size of the incline, arching might be an important effect. Indeed, if we compare the glass-glass and polystyrene-polystyrene interactions, the coefficient of dynamic friction is smaller in the second case, and being so small its density, it will be easier to break the arching expelling the polystyrene beads from the monolayer.

The movement of the beads starts as a pure rolling, and the increase of the intruder's mass implies the increase of the acceleration. Once the sliding starts, the increasing of acceleration slows down, due to the friction, and eventually gets constant. For the larger masses this has a reduction, probably due to the deformation of the spheres. In the other two materials, on the other hand, the movement starts at bigger masses, due to the mass of the beads (see Table I), so the first part of the corresponding curve for the polystyrene beads is very hard to observe, and also the final saturation, which could arise at masses above 400 g, unfeasible for the performed experiments.

As it could be expected κ varies linearly with the mass of the intruder. In Fig. 5 this is clearly seen: the three curves κ vs M are almost parallel in the measurement interval.

The slope is in the three cases around 200 $\mathrm{cm/s^2}$, close to the expected value of $g \sin\theta = 232$ $\mathrm{cm/s^2}$. A closer look reveals another interesting fact: the three lines have a negative intersection. These should be equal to $-\frac{nm}{2} g \sin\theta$ and, in fact, the dependence of the experimental values follows approximately the expectations. In Table II the values of the slope, the intersection and their uncertainties, as well as the calculated value of the intercept are shown.

TABLE II. Linear fitting parameters of κ vs M.

Material	Slope ($\mathrm{cm/s^2}$)	Intercept (N)	Theory (N)
Polystyrene	193 ± 11	0.0010 ± 0.0012	0.00004
Tapioca	197 ± 13	0.0090 ± 0.0030	0.0015
Glass	210 ± 15	0.0130 ± 0.0060	0.00525

In order to obtain a quantitative sight of this situation, let us rewrite Eq. (7), introducing explicitly the values of acceleration a,

$$Ma + \eta v^2 = \left(M - \frac{nm}{2}\right) g \sin\theta \tag{9}$$

and combining this with the dependence of the final speed in the trajectory of length s with the average acceleration,

$$v^2 = 2as \tag{10}$$

we obtain

$$a = \frac{1 - \dfrac{nm}{2M}}{1 + \dfrac{2\eta s}{M}} g \sin\theta. \tag{11}$$

Here, s is the length of the ramp used to calculate the average acceleration, in this case 100 cm. In Fig. 3(a) the numerical results obtained with this equation are depicted for the three materials (continuous lines). Retrospectively, this good agreement supports the need of an average acceleration. A result obtained from Eq. (11) is that the intruder's acceleration will be zero if $M = \frac{nm}{2}$, i.e., when the intruder's mass equals half the mass of the beads below it.

The dependence of the intruder's acceleration with the angle, shown in Fig. 3(b), is also correctly described (dashed lines), considering that there is a change in the value of η. Equation (11) includes all the dynamics of interaction of the intruder with the beads, the collision among beads and the arching in the effective parameter η. This parameter is related with the characteristics of the beads through Eq. (6). Equation (11) also includes the dependence of the average acceleration with the length of the ramp used to compute it.

The results described so far clarify the influence of the dynamics of the beads on the intruder's movement. However, to better understand its dynamics, we perform a "microscopic" study of the beads filming from below, see the movie provided here [16]. In doing so, we digitalized the videos using ImageJ, obtaining the positions of the individual beads in each frame. In order to calculate x_0 we considered only the trajectories that fulfill the following two criteria: (a) the bead starts to move when the front of the disk reaches it. (b) The

bead moves bellow the disk during the time it moves a distance R. No other requirement is imposed. Two extreme situations arise: when a bead is jammed in a group of beads, or when it freely moves in a fluidized region.

Clearly, uncertainties should be important in the above measurements. To evaluate them, we proceed as follows: (a) in the measurement of x_0 for one bead, the uncertainty was taken as the average distance a bead moves between two consecutive frames. (b) Around 15 trajectories were taken in each video, and the uncertainty in the average x_0 is the linear composition of its statistical uncertainty and the largest of the uncertainties of all trajectories. (c) For each mass of the disk, three videos were recorded, and we calculated the weighted mean value of x_0, being the statistical weight the inverse of the uncertainty.

Surprisingly, in the range of intruder's masses from 10 to 40 g, the values of x_0 are constant (considering the experimental uncertainty). The values of x_0 and its uncertainties for the different materials are: $x_{0,EP}=(0.52\pm0.11)$ cm, $x_{0,T}=(0.43\pm0.12)$ cm, $x_{0,G}=(0.36\pm0.10)$ cm. The values of η calculated from the above numbers and Eq. (6), are: $\eta_{EP}=(0.0021\pm0.0007)$ kg/m, $\eta_T=(0.065\pm0.018)$ kg/m, and $\eta_G=(0.12\pm0.05)$ kg/m.

The calculated values for expanded polystyrene and tapioca beads are of the same order of magnitude of the values found from the fitting to Eq. (8), but for glass, the difference is more important.

From these facts, several conclusions can be drawn. First, as the values of x_0 and n are relatively close for all materials, the notorious difference of η for polystyrene when compared with the other two materials must be related with the only parameter that varies more than one order of magnitude: the density. Second, the approximate coincidence of η_{exp} and η_{th} for polystyrene and tapioca indicates that the suppositions of the model are closer to reality for these two materials. Regarding glass, the difference is more significant, meaning that our model is not appropriate for this material, where the enduring contacts and impacts among beads are more important.

The dependence of η with the radius of the beads in the model is not considered explicitly. If there is rolling but no sliding, the value of x_0 is always $R/2$, independently of the bead's radius. Of course, the greater the radius, the smaller the angle rotated by the bead. So, if friction among beads is present, the smaller the radius, the greater will be the lost of energy. It can be concluded that in the realistic case, beads of smaller radius will have smaller acceleration. Supplementary measurements performed in beads of expanded polystyrene of smaller radius confirm this idea.

We also measured the linear mean speed of the beads in the following way: the visual field of the camera is divided in three separated areas, each of them larger than the diameter of the intruder, and select five different trajectories in each area. Then, the mean square speed is calculated. It is also possible to determine the average number of beads n below the disk while it slides down the incline. Considering the relation of the mass of the intruder over the average number of beads below it a measure of pressure, and the mean square speed a "temperature" of the monolayer, a diagram can be constructed. This is shown in Fig. 6(a). Here we can also

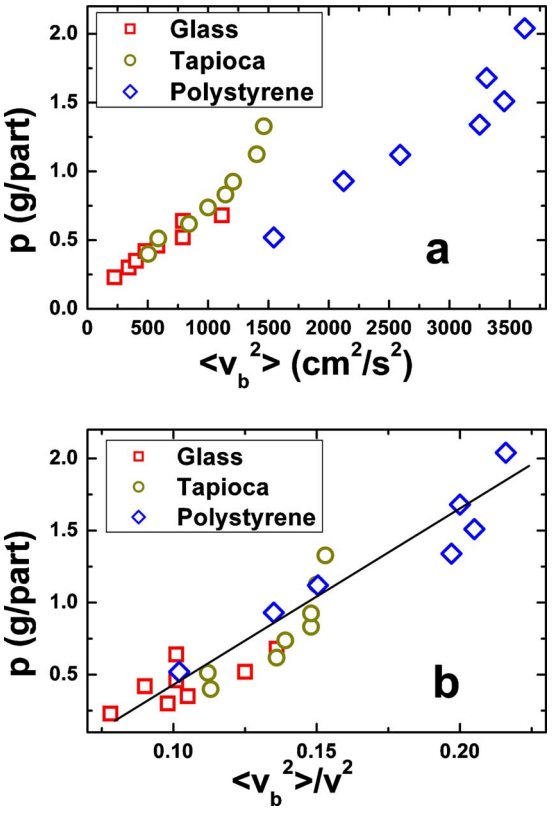

FIG. 6. (Color online) (a) Dependence of the pressure, defined as the ratio of the mass over the mean number of beads, with the mean square speed of the beads below the intruder. (b) Dependence of the pressure with the mean square speed, normalized to the mean square speed of the intruder. Continuous line is a guide to the eyes.

observe different behaviors when comparing the three different beads. Note, for instance, that although in the polystyrene beads the transfer of energy from the disk to the beads is very small, the average speed of the beads is large.

There is also another factor that influences the results depicted in Fig. 6(a): the fluidization of the beads. In Table I the values of the filling factors before and during the pass of the intruder are shown. It is easy to see that for glass an almost crystalline state is preserved, with an almost unchanged particle density close to the maximum packing fraction. But for tapioca and polystyrene beads, the filling factor has a notorious reduction. This implies a greater average distance between beads, an therefore a smaller number of impacts among beads and longer free paths, which determines a very low lost of energy. This can be seen when looking at the videos taken from bellow. If we return to Fig. 6(a), it is easy to see that in order to obtain in glass or tapioca beads a fluidization similar to that of polystyrene the pressure must increase enormously. This means that either the packing fraction of the beds must be lowered (keeping the mass of the intruder constant) or the mass of the intruder increase. It is important to note that in tapioca beads, although there is an important fluidization, the density of the beads is considerably higher than that of polystyrene, and, as a result, the interaction of the intruder and the beads implies the lost of energy and less acceleration.

If we scale the mean square speed of the beads with the square of the average speed of the intruder in the region of observation, a good collapse of the data is found, see Fig. 6(b). This surprising result might be expressed with the following motto: fluidize to lubricate. In fact, an intruder that moves on a monolayer of beads does it fast if it employs very low energy to fluidize the medium underneath. In other words, the intruder must be able to disrupt, using a little of its energy, the crystalline phase of the monolayer in order to freely move. Again, the collapse of the points in Fig. 6(b) means that a monolayer of denser beads (in this work tapioca or glass beads) would be as good lubricant as a monolayer of very light beads (in this work polystyrene beads) if somehow an intruder sliding on it is able to fluidize it using a small amount of its energy. It is important to remark the close analogy this phenomenon has with the phenomenon of sliding on ice, where surface melting (produced by pressure and friction) is crucial to promote slipperiness [17].

A quantitative description of this result can be done considering the dynamics of the intruder and the beads. Let us consider that while moving below the intruder, the beads do not interact among them. The system of equations that relates the movement of one bead and the movement of the intruder is

$$Mg \sin\theta - f_r = Ma, \tag{12}$$

$$mg \sin\theta + f_{r1} - f_{r2} = ma_b, \tag{13}$$

$$f_{r1}R_b + f_{r2}R_b = I\alpha. \tag{14}$$

Here f_{r2} represents the friction of the bead with the incline, a_b is the acceleration of the bead, I and α the inertial moment and angular acceleration, respectively. Using these equations, and Eq. (2), considering the possibility of rolling and sliding in both interfaces (intruder and ramp), and defining $t=1+\frac{2}{5\chi}$, $\chi=\frac{a}{\alpha R_b}\geq 1$; $p=\frac{M}{n}$, it is possible to find that

$$p = \frac{tm}{4x_0(g\sin\theta - a)}\langle v_b^2\rangle - \frac{mg\sin\theta}{2(g\sin\theta - a)}, \tag{15}$$

where $\langle v_b^2\rangle$ is the mean square speed of the beads. Denoting by l the distance from the beginning of the ramp to the mean position of the visual field of the camera in the experiment, it is easy to see that $a\approx\frac{v^2}{2l}$, so Eq. (15) can be transformed into

$$p = \frac{ltm}{2x_0\left(\frac{g\sin\theta}{a}-1\right)}\frac{\langle v_b^2\rangle}{v^2} - \frac{mg\sin\theta}{2(g\sin\theta - a)}. \tag{16}$$

In the two equations above l, g, θ, and m are constants. The magnitude of t and x_0 vary, but in an approximately equal amount: if sliding increases, both t and x_0 diminish. So the value of acceleration is the defining parameter in Eqs. (15) and (16). For the polystyrene beads, in the range of masses depicted, the acceleration is almost constant, so it is easy to understand the linear behavior obtained in Fig. 6(a). For tapioca, acceleration varies with the intruder's mass, and this affect the linearity, being the curve steeper with the increase of acceleration. For glass we find a linear behavior, which is counterintuitive, because also in this case the acceleration increases with the mass. But for these beads, due to the value of the filling factor (see Table I) the friction and the impacts among beads must be considered, and Eqs. (15) and (16) lost applicability, though gives an approximate description of the energy transfer.

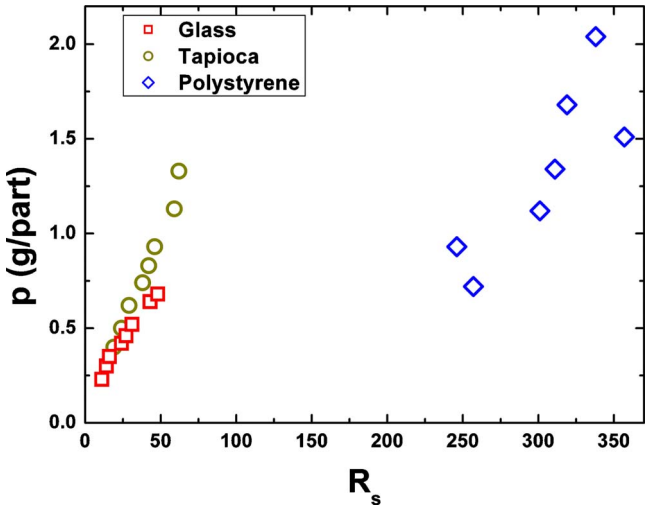

FIG. 7. (Color online) Dependence of the pressure with the sliding Reynolds number (see text for definition), for the three materials.

To understand the transfer of energy between the intruder and the beads, a sliding Reynolds number R_s can be defined. Following the general ideas about this kind of numbers, it can be defined as the ratio between the inertial and the frictional forces,

$$R_s = \frac{E_c}{W_{fr}}. \tag{17}$$

In this equation E_c is the kinetic energy of the intruder and W_{fr} is the work of the frictional force over the intruder, which is calculated over a characteristic length of the system: in this case the diameter of the intruder. Figure 7 depicts the dependence of pressure with R_s. The fluidized state is characterized by high R_s numbers, while highly dissipative states by $R_s<100$.

Using Eqs. (12)–(14), and an analysis similar to the one used to obtain Eq. (15), it is possible to find that

$$p = \frac{md(ta - g\sin\theta)}{2gh}R_s + \frac{md(ta - g\sin\theta)}{2gd\sin\theta}. \tag{18}$$

Here h is the height descended by the intruder performing a linear displacement l equal to the diameter of the intruder. From the details of the intruder's movement described above, it is easy to state that in the polystyrene bed the ratio has its greatest values, due to the fact that the dissipation of energy is smaller. That is related with two main facts: first, due to the small density of the beads, it is easier to push some beads out and obtain the dilatation necessary for the fluidization. Once the bed is fluidized, friction between grains is almost eliminated, and the dissipation of energy gets smaller. Second, all the experiments are performed for angles smaller than the critical one, so for the intruder start to moves (and, in general, to accelerate) it is necessary that part

of the potential energy of the intruder be transferred to the beads. And, again, this is easier for the polystyrene beads.

IV. CONCLUSIONS

We have studied the lubrication properties of a monolayer of beads on the displacement of an intruder moving on it. We find that the low density of the beads is crucial to obtain a reduced friction. Our results also teach us that the low density of the beads induces a bed fluidization, provoking in turn a greater acceleration of the intruder. When compared with the other denser materials, the contrast is more than evident. The lighter the beads, the sooner the rheology starts to be dominated by the rolling of the grains and the sliding of the intruder above them, being less important the friction and the collisions among grains.

ACKNOWLEDGMENTS

This work has been supported by Conacyt, Mexico, under Grants No. 46709 and No. 101384. F.P.V. wishes to acknowledge support by Conacyt, Mexico. A.J.B.L. thanks CINVESTAV IPN. We thank E. Altshuler (University of Havana) for useful comments and discussions.

APPENDIX

In order to determine the friction acting on the intruder according to Eq. (2), let us consider that a bead initially at rest is reached at t_0 by the intruder moving down the heap and after a time interval δt the bead moves a distance x_0 and reaches a speed v, while the intruder moves a distance R. Considering the forces acting on the bead, the theorem of work and energy states

$$W_{f_{r1}} + W_{f_{r2}} = \Delta E_c + \Delta E_{cr} + \Delta E_{pg}. \tag{A1}$$

Here W_{f_r} represents the work of the force and its momentum. Then

$$f_{r1}x_0 + \tau_{f_{r1}}\Delta\alpha - f_{r2}x_0 + \tau_{f_{r2}}\Delta\alpha = \frac{1}{2}mv_b^2 + \frac{1}{2}I\omega^2 + mg\Delta h \tag{A2}$$

where $\Delta h = x_0 \sin\theta$, and the angle rotated by the bead is $\Delta\alpha = \frac{x_0}{R_b}$. Considering that the bead is rolling without sliding, we obtain

$$2f_{r1}x_0 = \frac{7}{10}mv_b^2 + mgx_0 \sin\theta. \tag{A3}$$

We termed $\xi = \frac{R}{x_0}$. It is easy to understand that also $\xi = \frac{v}{v_b}$, thus

$$f_{r1} = \frac{7}{20}m\frac{v^2}{\xi^2 x_0} + \frac{1}{2}mg \sin\theta. \tag{A4}$$

From Eq. (A4) it follows Eq. (3).

[1] S. Dorbolo, Eur. Phys. J. E **17**, 77 (2005).
[2] T. Scheller, C. Huss, G. Lumay, N. Vandewalle, and S. Dorbolo, Phys. Rev. E **74**, 031311 (2006).
[3] J.-C. Tsai, W. Losert, G. A. Voth, and J. P. Gollub, Phys. Rev. E **65**, 011306 (2001).
[4] R. Candelier and O. Dauchot, Phys. Rev. Lett. **103**, 128001 (2009).
[5] L. Quartier, B. Andreotti, S. Douady, and A. Daerr, Phys. Rev. E **62**, 8299 (2000).
[6] O. Herbst, R. Cafiero, A. Zippelius, H. J. Herrmann, and S. Luding, Phys. Fluids **17**, 107102 (2005).
[7] D. W. Howell, R. P. Behringer, and C. T. Veje, Chaos **9**, 559 (1999).
[8] S. Luding, R. Cafiero, and H. J. Herrmann, in *Granular Dynamics*, edited by T. Pöschel and N. V. Brilliantov, Vol. 624 of Springer Lecture Notes in Physics (Springer, Berlin, 2003), p. 293-316.
[9] A. Puglisi, F. Cecconi, and A. Vulpiani, J. Phys.: Condens. Matter **17**, S2715 (2005).
[10] S. B. Savage, J. Fluid Mech. **377**, 1 (1998).
[11] A. Baldassarri, F. Dalton, A. Petri, S. Zapperi, G. Pontuale, and L. Pietronero, Phys. Rev. Lett. **96**, 118002 (2006).
[12] F. Pacheco-Vázquez and J. C. Ruiz-Suárez, Phys. Rev. E **80**, 060301(R) (2009).
[13] D. E. Shaw and F. J. Wunderlich, Am. J. Phys. **52**, 997 (1984).
[14] J. Solá de los Santos, R. Fernández Cruz, and J. L. Hernández Pérez, Rev. Esp. Fisiol **22**, 47 (2008).
[15] L. S. Tsimring and D. Volfson, in *Powder and Grains, Rotterdam, The Netherlands, 2005*, edited by R. García-Rojo, H. J. Herrmann, and S. McNamara (AA Balkiema Publishers, Rotterdam, The Netherlands, 2005), pp. 1215–1223.
[16] See supplementary material at http://link.aps.org/supplemental/10.1103/PhysRevE.82.031304 for a movie showing the bottom view of the ramp covered by a monolayer formed by three materials used in our study, while the intruder slides above it.
[17] R. Rosenberg, Phys. Today **58** (12), 50 (2005).